Highly Porous and Drug Loaded Amorphous Solid Dispersions Microfiber Scaffolds of Indomethacin prepared by Melt Electrowriting

Larissa Keßler[1], Zeynab Mirzaei[1], Juliane C. Kade[1, 2, 3], Robert Luxenhofer[1]

L. Keßler, Z. Mirzaei, J. C. Kade, R. Luxenhofer

[1] Soft Matter Chemistry, Department of Chemistry, and Helsinki Institute of Sustainability Science, Faculty of Science, University of Helsinki, 00014 Helsinki, Finland

L. Keßler, ORCID: 0000-0001-9041-612X

Z. Mirzaei, ORCID: 0000-0003-1534-3826

J. C. Kade, ORCID: 0000-0003-4210-3932

R. Luxenhofer, ORCID: 0000-0001-5567-7404

J. C. Kade

[2] Polymer Functional Materials, Chair for Advanced Materials Synthesis, Department of Chemistry and Pharmacy, Julius-Maximilians-University Würzburg, Würzburg, Germany.

J. C. Kade

[3] Department for Functional Materials in Medicine and Dentistry at the Institute of Functional Materials and Biofabrication, Julius-Maximilians-University Würzburg, Pleicherwall 2, 97070 Würzburg, Germany.

Correspondence to:

Prof. Dr. R. Luxenhofer: robert.luxenhofer@helsinki.fi

Keywords:

amphiphilic block copolymer, poly(2-oxazoline), poly(2-oxazine), drug formulation, electrohydrodynamic direct writing

Abstract

Melt electrowriting (MEW) is an additive manufacturing technology enabling the production of highly porous microfiber scaffolds, suggested in particular for use in biomedical applications, including drug delivery. Indomethacin (IND) is a non-selective anti-inflammatory drug, for which sublingual delivery could offer advantages such as rapid absorption by the veins in the mouth floor while overcoming the side-effects of peroral delivery such as damage to gastrointestinal mucosa barrier. This study introduces MEW as a processing method to obtain rapid-dissolving drug releasing scaffolds, containing IND as a model drug, for sublingual drug delivery applications. For this, an amorphous solid dispersion of IND in combination of a novel poly(2-oxazoline) based amphiphilic triblock copolymer excipient is introduced, enabling ultra-high drug loading.

We prepared highly porous, melt electrowritten drug-loaded scaffolds with different polymer:IND w/w ratios up to 1:2 and assessed their morphology, amorphicity, and IND release rate. The results show completely amorphous dispersion of the polymer and drug after MEW processing resulting in smooth and uniform fibers, and rapid dissolution of the polymer.

These first water soluble melt electrowritten IND-loaded microfiber scaffolds break ground as a model for rapid sublingual delivery of ultra-high drug loaded amorphous solid dispersions.

Introduction

Sublingual or buccal drug delivery approaches have gained increasing attention due to the fast and direct drug uptake in the oral cavity. The sublingual route is known to be one of the most effective ones, as the drug is directly absorbed by the high number of capillaries below the tongue and effectively brought to the blood circulation.[1, 2] Additionally, sublingual drug-delivery systems are designed for the drug to avoid passing the gastrointestinal tract, reducing potential side effects of the drugs observed with common peroral delivery, such as gastrointestinal ulceration, and limitations of local acidic conditions, as well as enzymatic degradation.[3] Furthermore, these approaches simplify the uptake of the drugs, as they avoid potential swallowing difficulties[4] improving patient compliance.

Indomethacin (IND) is used as a model drug for the development of novel sublingual drug delivery approaches. This nonsteroidal anti-inflammatory drug is commonly used as a painkiller with an oral administration to reduce fever and swelling, as well as a medication to treat rheumatoid arthritis or osteoarthritis due to its strong action and high therapeutic efficacy in the body[5]. However, at the same time, its short half-life time and the associated repeated oral administration result in toxicity-issues toward the digestive system and kidneys as well as malaises like nausea, stomach pain, and diarrhoea which could be expected to be reduced by using sublingual delivery system.[6]

Maintaining drugs in their amorphous state improves the dissolution rate and oral bioavailability.[7] However, some limitations including recrystallization due to the physical instability of the amorphous state and residual micro-crystallinity of the drug can cause problems such as patient-to-patient variability.[8] This can be addressed and overcome via preparation of amorphous solid dispersions (ASD) using suitable excipients, e.g., through tuning the interactions between polymeric excipients and drug.[9] One well-known and widely used method to fabricate ASDs is hot melt extrusion (HME). This method involves melting and intensive mixing of the drug into the polymer matrix, resulting in the formation of a single phase.[10] There are numerous well-known and well-studied polymer excipients for the preparation of ASDs[11], such as poly(2-ethyl-2-oxazoline) and its structural similar polyvinyl pyrrolidone resulting in a better performance of the 2-oxazoline based polymer[12]. The selection of an excipient is not only based on the processability using a given method and the possibility of designing a controlled release from the amorphous formulation, but also the miscibility and possible interactions between drug and polymer play an important role.[13]

Previously, poly(2-oxazoline)/poly(2-oxazine) triblock copolymers have been employed very successfully in high drug loading formulations[14] with up to and more than 50 wt.% of drug.[15] Also, diblock, random and gradient copolymers from poly(2-oxazoline)s/poly(2-oxazine)s have been investigated as potential excipients[16] and some systems also allowed high drug loadings.[17]

Depending on the properties of the chosen polymer and drug, the drug loading capacity can be changed and adjusted to the required needs.[18] An amorphous blend facilitates a faster dissolution and drug release compared to crystalline drug loaded material, due to its higher free energy[19] achievable for example using melt processing techniques such as previously mentioned HME. Furthermore, drug delivery systems with a high surface area to volume ratio are also beneficial and favourable, because they can provide a high capacity of drug loading in addition to a fast dissolution due to their highly porous design.[20] Solution electrospun fibers containing drugs are already well studied as fast sublingual drug delivery systems due to their high surface area and exceedingly small fiber diameters showing great potential for this application.[2] In addition, they provide faster dissolution compared to films; however, the electrospinning technique requires (often toxic) solvents and the processed fibers are randomly oriented[21], limiting the degree of control over the morphology. Another method capable of producing fibers within the lower micron-range is called melt electrowriting (MEW), which electrostatically draws a polymer melt out of a syringe onto a computer-controlled moving collector without the need of (toxic) solvents. MEW is a high resolution additive manufacturing (AM) technology allowing accurate microfiber placement with fiber diameters commonly ranging between 5 µm to ~ 50 µm and production of unique printing patterns, as well as highly porous microfiber scaffolds.[22] This technique uniquely fills the fabrication gap between solution electrospinning and melt extrusion-based direct writing. The former produces sub-micron fibers with chaotic and uncontrollable fiber placement, while the latter allows good fiber placement but generates larger diameters, typically well of above 100 µm.[23] The high porosity and larger surface area of the MEW scaffolds compared to films or other 3D printed constructs benefits the use in a variety of biomedical applications, including tissue engineering[24, 25] and drug delivery [25, 26].

In this study, an amphiphilic triblock copolymer (pMeOzi-*b*-pPentOx-*b*-pMeOzi) has been synthesized and explored as an excipient to enable I) processing via HME and MEW, II) retaining fully amorphous character of the drug and III) allowing fast and complete dissolution of the incorporated drug (**Figure 1**).

For this purpose, pMeOzi-*b*-pPentOx-*b*-pMeOzi has been blended via HME with different ratios of IND, and these blends were processed using MEW for the first time (**Figure 1**). Furthermore, the influence of the drug-loading content on the processability was elucidated, and the blends and resulting drug-loaded fibrous scaffolds were investigated regarding their properties using scanning electron microscopy (SEM), thermogravimetric analysis (TGA), differential scanning calorimetry (DSC), and powder X-Ray diffraction (PXRD), as well as drug-release test.

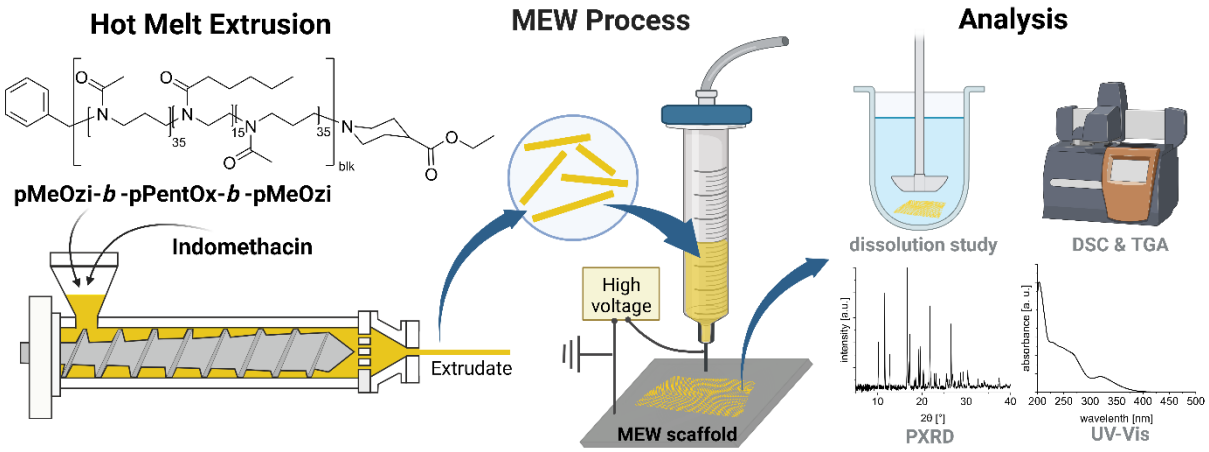

Figure 1. Schematic overview of this study. Blending of the triblock copolymer with indomethacin via hot melt extrusion and subsequent processing into 3D porous scaffolds using melt electrowriting for potential sublingual drug-delivery applications. Created with biorender.com.

2. Materials and methods

2.1. Source of materials

Indomethacin and benzylbromide were purchased from TCI chemicals (Zwijndrecht, Belgium), 3- amino-propanol, 2-amino-ethanol, acetonitrile, benzonitrile, 2-methyl-2-oxazoline, CaH_2 and zinc acetate dihydrate were obtained from Sigma-Aldrich (Helsinki, Finland) and used as received unless otherwise stated.

2-Methyl-2-oxazine and 2-pentyl-2-oxazoline were dried by refluxing over CaH_2 under inert atmosphere, followed by distillation prior to use. Benzonitrile was dried by refluxing over P_2O_5 under inert atmosphere, followed by distillation prior to use.

2.2. Synthesis of polymer

The monomers 2-methyl-2-oxazine (MeOzi) and 2-pentyl-2-oxazoline (PentOx) were synthesized following the procedure by Witte and Seeliger.[27] Detailed information about the synthesis can be found in the supporting information (**Table S1-2 and Figure S1-2**). Briefly explained, the respective nitrile, 3-amino-propanol for the synthesis of the 2-oxazines or 2-amino-ethanol for the synthesis of the 2-oxazolines, and catalytic amounts of zinc acetate dihydrate were mixed in a N_2 flushed flask and heated to 130°C under reflux for two days. The progress was controlled by ^{1}H NMR spectroscopy. After completion of the reaction, the PentOx mixture was dissolved in dichloromethane and washed with H_2O three times. The organic phase was dried with Na_2SO_4 and concentrated. The raw product was dried over CaH_2 and distilled under reduced pressure under N_2 atmosphere to yield the product as a colourless liquid. MeOzi was distilled directly out of the reaction mixture after completion of the reaction.

The polymer synthesis and workup procedures were carried out as described elsewhere.[28] Briefly, the initiator was added to a dried and N_2 flushed Schlenk flask and dissolved in the respective amount of solvent. The monomer MeOzi was added, and the reaction mixture was heated to 130°C and stirred until complete consumption of the monomer, as was monitored by ^{1}H NMR spectroscopy. After consumption of MeOzi, the mixture was cooled to room temperature and the second block, PentOx, was added. The mixture was heated to 130°C overnight. The same procedure was repeated for the third block MeOzi. After confirmation of monomer consumption by ^{1}H NMR, the polymerization was terminated by addition of ethylisonipecotate at 50°C for 4 h. The solvent was removed under reduced pressure and the residue was transferred into a dialysis bag (MWCO 1 kDa, cellulose acetate) and dialysed against deionized water for two days with several water changes. Afterwards, the solution was recovered from the bag and lyophilized. Further information can be found in the Supporting Information (**Table S3** and **Figure S3**).

2.3. Hot melt extrusion (HME)

HME was carried out on a ZE 9 HMI extruder (Three-Tec GmbH, Seon, Switzerland) at 100°C in all three heating zones to ensure the formation of a continuous filament. The screw speed was set to 25 rpm for the whole extrusion process. The total amount of polymer and IND used for each round was about 5 g which did not allow the use of continuous feeding. Therefore, manual feeding of the extruder had to be done to facilitate smooth, uniform and non-sticky extrudates with improved handling under cooled storage conditions prior to use due to the low T_g of the polymer.

2.4. MEW printing

A custom-built MEW printer similar to a previously described machine[29] was used in order to process the neat polymer and different ratios of polymer:IND extrudates. The 3 mL glass syringes (Poulten & Graf GmbH, Germany) were loaded with different materials and heated for a minimum of 30 minutes prior to printing until the bubbles within the melt dissipated. For all experiments, a nozzle tip with an inner diameter of 0.337 mm (23G) was used and manually grinded to a length of 13 mm. Other applied printing parameters are listed in **Table 1**.

Table 1. MEW printing parameters for the neat polymer and different polymer:IND ratios.

	$T_{syringe}$ [°C]	T_{nozzle} [°C]	voltage [kV]	pressure [MPa]	distance [mm]	speed [mm min^{-1}]
polymer:IND w/w 1:0	155	155	3.0-4.0	0.1	4	1500
polymer:IND w/w 2:1	140	140	2.5-3.0	0.1	4	1400
polymer:IND w/w 1:1	135	135	3.0-5.5	0.1	4	1000
polymer:IND w/w 1:2	130	130	2.5-4.5	0.1	4	700

2.5. Characterisation of the extrudates and scaffolds

2.5.1. Thermogravimetric analysis (TGA)

TGA of the polymers was performed using a Netzsch STA 449 F3 Jupiter instrument (Germany) under a N_2 atmosphere. The samples of about 5 mg neat polymer and polymer:IND w/w 1:1 extrudates were prepared in aluminium oxide crucibles heated to 140°C (10°C min^{-1}) and kept at constant temperature for 5 h and then, further heated to 900°C to detect the mass loss. The thermograms were evaluated using Origin software (OriginPro 2021. OriginLab Corp., Northampton, MA.).

2.5.2. Differential scanning calorimetry (DSC)

In order to evaluate the thermal behaviour of neat IND, polymer:IND extrudates and IND-loaded MEW printed scaffolds, DSC was conducted using DSC Q 2000 (TA Instruments, USA). Specimens of about 5 mg of each sample were prepared in aluminium pans, sealed and heated from 5°C to 200°C and subsequently cooled to −50°C at a linear rate of 10°C min^{-1} in a N_2

atmosphere. This cycle was repeated three times, i.e., heating to 200°C and further cooling to −50°C. In the final cycle, the samples were cooled from 200°C to the room temperature and the glass transition temperature (T_g), melting temperature (T_m) and enthalpy of fusion (ΔH_f) were determined. T_g was obtained from the inflection point of the second and third heating cycle and T_m is the onset of the endothermic curve in the first heating. ΔH_f was calculated by determination of the area bounded by the endotherm normalized to the mass of the polymer samples. The thermograms were evaluated using Origin software.

2.5.3. Powder X-Ray diffraction (PXRD)

Diffraction patterns of neat IND and polymer:IND extrudates and scaffolds were obtained using an EMPYREAN X-ray diffractometer (Malvern PANalytical, Espoo, Finland) equipped with a transmission measurement geometry at room temperature and voltage of 45 kV. Each sample was scanned between 5° and 40° 2θ with a step size of 0.013° 2θ and a step time of 49.47 s. The samples were grinded, placed between two slices of kapton tape and mounted on a transmission sample holder. The diffractograms were evaluated using Origin software.

2.5.4. Ultraviolet-visible (UV-Vis) spectroscopy

UV-Vis experiments were performed on a JASCO V-750 UV-Vis spectrometer (JASCO UK Ltd., UK) equipped with a JASCO CTU-100 water jacketed Peltier thermostat system at a wavelength of 320 nm and a temperature of 25°C. A standard curve for IND was obtained by quantifying known amounts (**Figure S4**). Data was analysed using the Origin software.

2.5.5. Rheology characterization

Rheological properties of the polymer and polymer:IND extrudates were characterized using a Discovery Hybrid Rheometer HR-2 (TA Instruments, USA) equipped with an Environmental Test Chamber (ETC), as well as with an air chiller system. The ETC is a high temperature oven that provides uniform and stable temperature during the measurements. The samples were prepared in a hot air oven (Hewlett Packard HP 5890 Series, Gas Chromatograph, Agilent Technologies, USA) using in-house teflon molds with diameter of 25 mm. A plate–plate setup and an upper 25 mm plate used for all the measurements. The behaviour of the prepared samples was tested for 5 h under constant dynamic-mechanical low-shear conditions. The frequency was set to 10 rad s^{-1} and the shear strain to 1%. In the same measurement, the behaviour of the complex viscosity during isothermal heating was observed. The temperature of the measurements was changed depending on the drug loading, to have similar temperatures as MEW printing procedure. Data was analysed using the Origin software.

2.5.6. Scanning electron microscopy (SEM)

The diameter, morphology and alignment of the MEW-processed fibers were characterized using field emission scanning electron microscopy (FESEM) (Hitachi S-4800, Hitachi Ltd., Japan). Before imaging, all samples were sputter coated with a thickness of 5 nm Au/Pd to create a conductive surface (Cressington 208HR, Ted Pella Inc, USA). An accelerating voltage of 5 kV was applied for imaging and ≈50 fibers were analysed using ImageJ software[30] to determine the average fiber diameter for each sample.

2.5.7. Dissolution tests

Dissolution tests were performed on an in-house built Unites States Pharmacopeia (USP) dissolution apparatus 2 with rotational speed of 50 rpm and temperature set to 37°C. The dissolution medium was chosen to be 250 mL phosphate buffered saline (pH = 7.4) (Ph. Eur.). The printed scaffolds were weighted and added to the dissolution medium. At set time points between 0 and 30 min, samples of 3 mL were removed, and the medium was refilled with 3 mL fresh buffer solution (37°C) every time. The amount of dissolved IND was investigated by UV-Vis spectroscopy at these time points. The data was evaluated using Origin software.

2.5.8 Size exclusion chromatography (SEC)

SEC was measured with a Waters Acquity APC system, equipped with Acquity Column Manager – S, Sample Manager – pFTN, Isocratic Solvent Manager, Acquity RI Detector and Acquity TUV Detector (Waters Corporation, USA). The used columns are Acquity APC XT 45, 125 and 200. Dimethylformamide (DMF, Fisher Scientific) was used as eluent with a flow speed of 0.6 mL min^{-1} and at a temperature of 40°C. The system was calibrated with PMMA standards (Polymer Standard Service). The data was analysed using the software Empower 3 and Origin software.

2.5.9 Nuclear magnetic resonance spectroscopy (NMR)

^{1}H NMR spectra were measured with a Avance III 500MHz spectrometer from Bruker Biospin (Germany) at a temperature of 25°C (298 K). The spectra were calibrated on the residual protonated solvent (CD_2Cl_2) signal (5.32 ppm). The data was evaluated using Bruker Topspin 4.1.3.

2.5.10 Glass transition predictions by Gordon-Taylor equation

The glass transition temperatures of homogenous mixed amorphous solid dispersion of the synthesized polymer and IND was calculated for different polymer:IND ratios ($T_g(x_{IND})$) using the Gordon Taylor equation:

$$T_g(x_{IND}) = \frac{x_{IND}\,T_{g,IND} + K(1-x_{IND})T_{g,Poly}}{x_{IND} + K(1-x_{IND})} \quad (1)$$

with the glass transition of the neat polymer $T_{g,Poly}$ and neat IND $T_{g,IND}$, and the weight fraction of IND x_{IND}, respectively. The parameter K was calculated from equation (2) where $\Delta C_{p,Poly}$ and $\Delta C_{p,IND}$ are the amplitude of the C_p jump at the T_g determined for the neat polymer and the neat IND, respectively.

$$K = \frac{\Delta C_{p,Poly}}{\Delta C_{p,IND}} \quad (2)$$

3. Results and discussion

3.1. Synthesis and characterization of the polymer

The synthesis of the ABA triblock copolymer, comprising 2-methyl-2-oxazine (MeOzi) as block A and 2-pentyl-2-oxazoline (PentOx) as block B, was performed via living cationic ring opening polymerization (LCROP) and the product was characterised by ^{1}H NMR spectroscopy and SEC (**Figure S3A-B**). During synthesis, a colour change of the reaction mixture from colourless to orange was observed, suggesting some undesired side reactions. Also, the required reaction time of the hydrophilic block was significantly longer than 2-methyl-2-oxazoline (MeOx), due to the lower reactivity of MeOzi.[31] Important to note, we used benzylbromide as an initiator, as the polymerization with the commonly used methyltriflate was not successful (no detailed analysis was conducted at this point). However, the change of the initiator coincided with a higher dispersity (Đ= 1.45) than typically obtained for the LCROP. This notwithstanding, the thermal behaviour of the polymer is crucial for the current contribution and was studied by DSC measurements. In the second heating cycle (**Figure S3C**), the polymer shows a T_g at 27 °C, crystallization at 56 °C and T_m at 141 °C. Room temperature PXRD pattern (of unheated polymer) indicates the amorphous nature of the polymer. The DSC thermogram and PXRD pattern lead to the assumption that a first heating above 56 °C is necessary to induce partial crystallization of the polymer yielding a cold crystallization peak upon cooling and a T_m on second heating.

3.2. Preparation and characterisation of polymer:IND extrudates

Since the interest of this study was the fabrication of a (rapidly) dissolvable triblock polymer formulated with IND (**Figure 1**), blending of both components played a crucial role, especially in regards to obtain and retain both components in the amorphous state to favour a fast drug release and uptake.[18] For the blending process of the polymer and IND, manually grinding and mixing using a mortar was tested, but this proved impractical. The polymer was too viscous and sticky to allow effective blending. In contrast, the low T_g of the polymer makes it a good candidate for HME. Here, only a moderate temperature would be needed during the extrusion process so that the IND can be mixed in. The weight ratio between polymer and IND can be easily altered by using different ratios of the respective compounds in the process.

As mentioned before, to reduce the applied heat as far as possible, the polymer and drug were extruded in different weight ratios using HME. Since the extrusion was done far below the T_m of IND (160°C) and only for a brief time (approx. 10 min), some residual crystalline drug was still present and visible in the extrudates (**Figure S5**). This was also analysed by DSC and PXRD analysis of the resulting extrudates. In particular, the first heating cycle of the DSC was analysed which is usually not discussed due to the existence of polymer's thermal history that

should be removed by heating.[32] However, in this study the residual crystallinity of IND is only visible in the first heating curve of the DSC measurement, because it has a very good glass stability (Class III compound)[33] and usually does not crystalize in the used DSC protocol. Furthermore, as the polymer and IND are heated higher than the extrusion temperature in the DSC run to reach the T_m of the drug, the two components can then merge and the solubility of the drug in the polymer matrix increases. Additionally, if all of the drug gets solubilized while heating, subsequently no melting will be observed[34], as observed for the samples with polymer:IND w/w ratios of 1:2 and 1:1 (**Figure 2A**). However, a residual broad endothermic transition between 110 and 140°C can be observed for the sample containing higher amount of polymer (polymer:IND w/w 2:1) followed by two sharp peaks at 145 and 153°C.

To analyse the residual crystallinity of the samples without applying additional thermal energy, PXRD measurements of the extrudates were carried out (**Figure 2B**). The potential reflexes from residual crystallinity peaks are highlighted, and residual crystallinity is minute, but not entirely absent, although it is difficult to determine these peaks due to the low signal to noise ratio within the PXRD patterns.

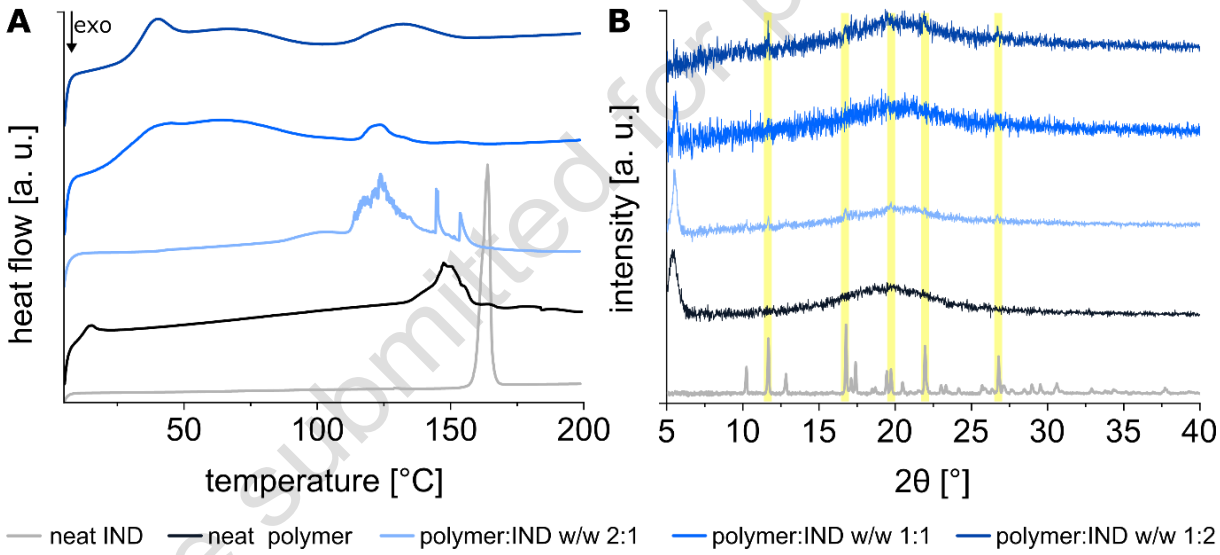

Figure 2. A) First heating curves of the DSC measurements for IND and the polymer:IND extrudates with ratios (w/w) of 1:2, 1:1 and 2:1, respectively. B) PXRD pattern of the neat IND and polymer, as well as the extrudates with different polymer:IND w/w ratios; 1:2, 1:1 and 2:1, respectively, measured at RT. Yellow lines highlight the residual crystallinity peaks.

The resulting thermal properties of the neat polymer and the polymer:IND extrudates (**Table 2**), indicate an influence of drug loading on the T_g of the extrudates as it increases with higher drug concentration. The T_g for each sample was also calculated using the Gordon Taylor equation (**Equation 1**)[35] and the calculated values are lower than the experimentally obtained ones for all polymer:IND ratios. This positive deviation from the theoretical T_g could be attributed to a higher number and strength of interactions between the polymer and the drug

in the mixture than in the individual components due to for example hydrogen bonding between the amide moieties in the polymer and the carboxylic acid of IND.[36]

Table 2. Thermal properties of the neat polymer and drug, as well as the extrudates with different polymer:IND ratios. T_g^1 was taken from the 2nd and 3rd heating cycles of DSC measurements (**Figure S6**). The T_m and ΔH_f was taken from the 1st heating cycle for IND and from 2nd and 3rd heating cycle for the polymer. T_g^2 was calculated by Gordon Taylor equation.

	T_g^1 [°C]	T_g^2 [°C]	T_m [°C]	ΔH_f [J g^{-1}]
polymer:IND w/w 1:0	27	27	141	11.84
polymer:IND w/w 2:1	36	32	130	0.75
polymer:IND w/w 1:1	37	35	-	-
polymer:IND w/w 1:2	42	37	-	-
polymer:IND w/w 0:1	43	43	160	108.9

3.3. MEW printing and characterisation of scaffolds

To overcome the remaining crystallinity of IND within the polymer matrix, the DSC measurements showed that simply remelting the extrudates resolved this issue. Apart from the amorphous character, a second parameter is critical to facilitate rapid dissolution - a high surface area. For this, highly porous microfiber meshes consisting of small diameter fibers offer a higher surface area compared to solid films and should be ideal for an accelerated drug release. As mentioned before, MEW has been chosen here to fabricate such controlled microfibrous scaffolds without the use of toxic solvents.

Therefore, the MEW processability of the ABA triblock copolymer, MeOzi-*b*-PentOx-*b*-MeOzi, and the resulting extrudates consisting of different polymer:IND w/w ratios of 2:1, 1:1 and 1:2, were investigated. The neat polymer was processable at a syringe and nozzle temperature of 155 °C. When processing polymer:IND extrudates, with increasing drug content, the processing temperature could be decreased down to 130 °C for the blend containing polymer:IND w/w ratio of 1:2 (**Table 1**).

Due to the fast solidification rate of the melts, as previously shown by Nahm *et al.* for poly(2-ethyl-2-oxazine) (PEtOzi),[37] a small distance of 4 mm between the print head and the collector is required to enable sufficient direct writing. Furthermore, fiber pulsing after 5 to 10 layers was observed and therefore, manual adjustment of the applied voltage while printing was needed to enable accurate fiber placement with homogenous diameters and reduce fiber pulsing or jet break within higher layers.

The resulting fibers exhibit a smooth fiber morphology, and for direct-written neat polymer a reasonably good stackability and alignment of the MEW fibers (**Figure 3**) was achieved for

20 alternating layers while for the different polymer:IND ratios 15 alternating layers could be printed. All processed polymers and polymer:IND blends show round-shaped fibers without flattening in-between the layers. The fiber diameters of all processed materials are between 25 to 50 µm (**Figure 3**). However, no general trend is visible as the printing parameters were individually adjusted for the neat polymer and the polymer:IND blends (**Table 1**), significantly influencing the resulting fiber diameters. By increasing the hydrophobic drug content, the stackability of the fibers deteriorates leading to bigger gaps between the stacked layers. This might be caused by increased repulsion between the hydrophobic drug particles and therefore, processed fibers. The distribution of IND in the printed scaffold was investigated by placing the scaffold under UV light, which revealed in a homogenous fluorescence emission (**Figure S7**).

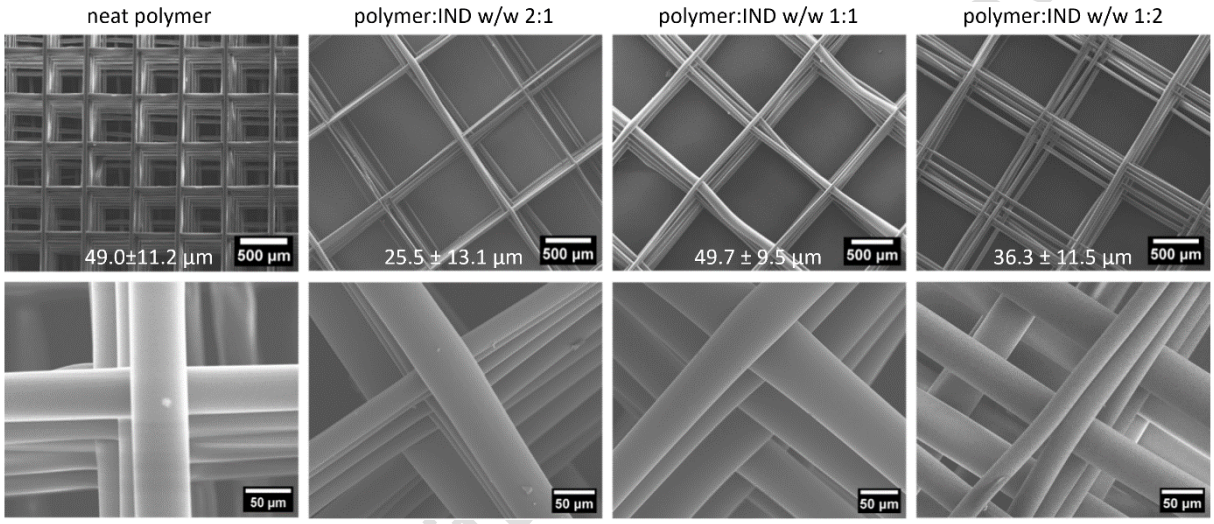

Figure 3. SEM images of the MEW scaffolds fabricated using neat polymer and different polymer:IND ratios (w/w) of 2:1, 1:1 and 1:2, respectively. First row showing overview images, as well as the average fiber diameter results and second row indicating magnified view, highlighting the smooth fibers surfaces and stackability of all processed materials.

Using IND as oral capsules or suspension, the drug loading is commonly based on release rate, age, type and severity of the patient's condition and is around 20 - 100 mg per unit.[38] However, in freeze-dried sublingual tablets, the drug loading has been investigated at around 25 mg per unit.[3] When processing the blend polymer:IND 1:2 (w/w) into scaffolds with 15 alternating layers, the sample weight is around 90 mg and therefore, drug loading is about 60 mg. As MEW is a multi-parameter process and the scaffold design is controlled via the G-code, the dosage of IND in MEW printed scaffolds could be readily adjusted by, for example, changing the fiber diameter as required. The diameter can be varied via the applied pressure and/or the printing speed. Furthermore, the scaffold design can also be altered regarding the fiber spacing and the number of stacked layers resulting in more direct-written material and, respectively, in higher drug-content per volume.

To further improve the layer stacking and scaffold height, a MEW printer with automatically adjustable voltage and Z-height of the print head would be needed, as demonstrated by Wunner and co-workers. [29]

While printing, we observed a colour change from yellow to brown of the drug loaded extrudates over time (**Figure S8**). IND is known to be easily degradable above its T_m, therefore, a possible degradation was investigated by TGA measurements (**Figure 4A**). The TGA graph of the polymer showed an initial mass loss of 5% while heating to 140 °C, followed by a plateau during the isotherm.

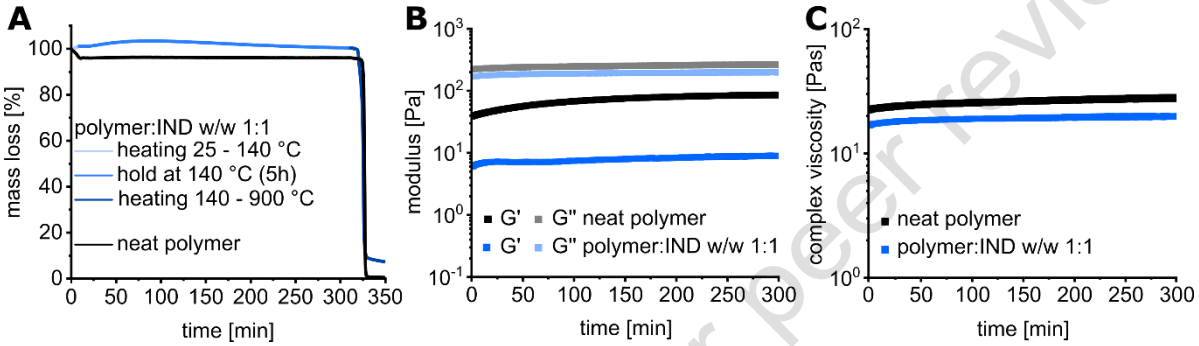

Figure 4. A) showing the TGA measurement of the neat polymer and the polymer:IND extrudate (w/w) 1:1, B) the rheology time sweep displaying storage modulus G' and loss modulus G'' and C) the rheology time sweep displaying the complex viscosity over the measurement time.

The initial mass loss could be caused by evaporation of water as the used polymer is hygroscopic and was not dried specifically before the measurement. Increasing the temperature to above 350 °C, degradation of the polymer takes place, as evidenced by the mass loss. A different behaviour was observed for the extrudates. During the initial heating process and the isothermal heating an increase in mass, albeit it minor, was observed. The mass gain might be due to oxidation or measuring artefact, as the polymer is expected to be stable up to 350 °C. Similar results have been observed for TGA measurements of MEW-processed samples using PVDF.[23] Further heating to 900 °C, resulted in a mass loss from 99 to 9 % due to the degradation of the polymer.

The thermal behaviour and the resulting potential changes within the polymer:IND extrudates were also investigated by melt rheology (**Figure 4B**). The value for G'' (loss modulus) is constant at 250 Pa for the neat polymer sample during the whole measurement and at 190 Pa for the polymer:IND extrudate. A slightly different behaviour can be observed for G' (storage modulus). During heating, a moderate but continuous increase in G' is visible. The increase in elastic strength can be explained by additional molecular entanglement of the polymer chains over time. This effect is more pronounced when measuring the neat polymer. The drug acts as a plasticizer, reducing viscosity in the molten blend (**Figure 4C**), correlating

with the decreasing MEW-processing temperatures with increasing drug content (**Table 1**). Even at a lower printing temperature, the viscosity of the melted blend is lower than that of the neat polymer. Importantly, no major change in viscosity was observed during isothermal heating. Apparently, potential degradation of the drug does not have a marked influence on the viscosity of the blend, and therefore also not on the printing process. Nevertheless, degradation of the drug after being heated to 140°C in the printer for several hours could be verified by ^{1}H NMR measurements (**Figure S9**). A possible degradation mechanism induced by thermal treatment is for instance decarboxylation.[39]

The MEW printed scaffolds were analysed by DSC and PXRD to ensure the amorphous state of the drug (**Figure 5**). As already mentioned before, the signal to noise ratio of the PXRD patterns makes it difficult to exclude minute crystalline components, especially since the diffractograms of polymer:IND scaffolds show more noise than those of the neat polymer. However, in contrast to before MEW printing, there is no obvious residual crystallinity left in the structure directly after printing. This could be confirmed by DSC measurements as well. In the first heating curve of the scaffolds, in contrast to before MEW, no melting peak of IND is visible.

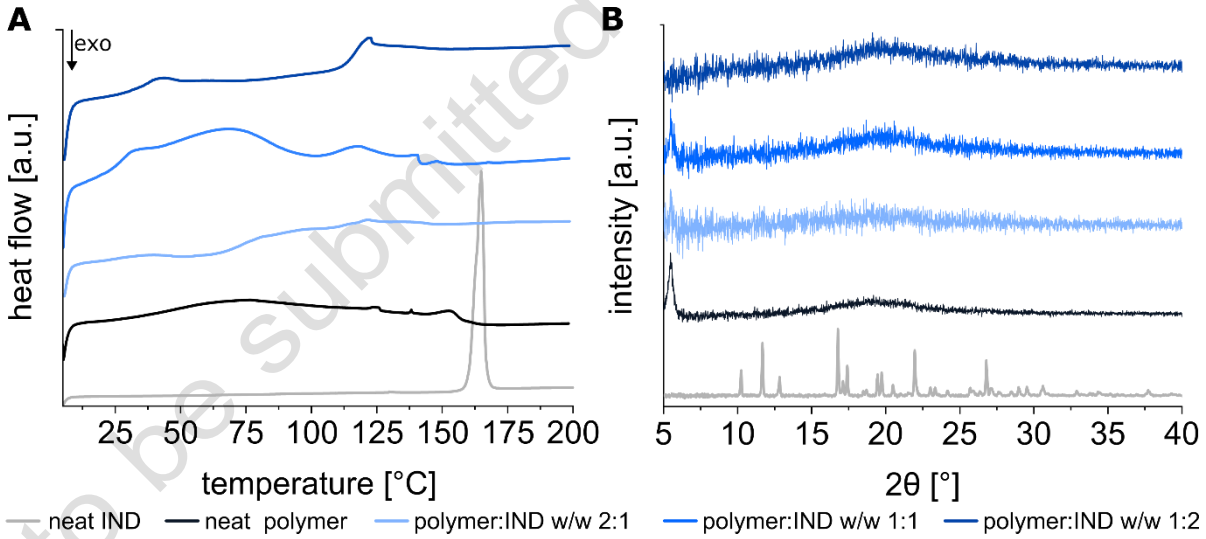

Figure 5. A) DSC thermograms of MEW printed scaffolds (1st heating) and B) PXRD pattern of MEW scaffolds fabricated using the neat polymer and polymer:IND blends with ratio (w/w) of 2:1, 1:1 and 1:2, respectively.

After determining the solid-state properties of the drug loaded scaffolds, their dissolution behaviour was investigated. As there is no standardized approach to test the dissolution properties for sublingual dosage forms, the study was done similar to a previously published approach by Lopez and co-workers[40] below the solubility limit of IND in PBS (223 mg mL^{-1}). [41]

The MEW-processed scaffolds fabricated using the polymer:IND blends of 1:1 and 1:2 (w/w) clearly showed a different dissolution behaviour (**Figure 6**). The samples consisting of polymer:IND 1:1 (w/w), dissolve faster, within about 2.5 min they reach a plateau at 80% released drug after which drug concentration stays nearly constant over the remaining experiment duration. In contrast, the scaffolds of polymer:IND 1:2 (w/w) show slower dissolution, even though almost 75% of the drug is still released in less than 5 min. At this point, we attribute the fact in one case the drug loading levels off at 80% and at almost 120% at inhomogeneities in drug content of individual scaffolds and differences in drug stability for the different drug contents.

Overall, using the multi-parameter process, i.e., MEW, to process IND-loaded scaffolds for sublingual drug delivery applications enables the fabrication of adaptable patient-specific drug-loading. This could potentially be done by adjusting for example the nozzle size, the resulting fiber diameter and the number of stacked layers leading to different weights of incorporated and delivered drug, as previously discussed.

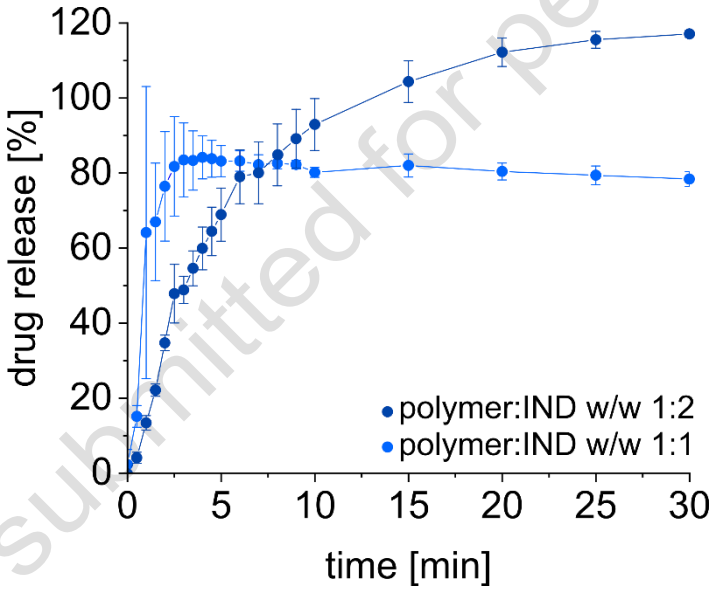

Figure 6. Dissolution profile of the drug loaded MEW printed scaffolds (n=3) with polymer:IND w/w ratio of 1:1 and 1:2 in 250 mL PBS (pH = 7.4).

Although these first MEW printed drug loaded scaffolds using an ABA triblock copolymer for sublingual drug application seem to be promising, this method has some limitations. The combination of two high temperature methods (HME and MEW printing) limit the choice of drug, as it needs to be sufficiently temperature stable. Also, the total amount of drug that can be printed in suitably sized scaffolds is somewhat limited (here about 60 mg), which makes the use of a highly potent drug necessary. Additionally, the T_g of the used polymer needs to be relatively low to allow printing below the degradation temperature of the drug, in the case presented here, the T_g of the polymer is 27 °C. However, to prevent recrystallization of the

drug, a generic rule is that the T_g of the polymer should be around 50°C above the storage temperature. Nevertheless, as the long-term stability was not tested within this study, the influence of the low T_g on the recrystallization behaviour of the drug, as well as the dissolution behaviour of the scaffold after storage is not clear. It should be noted, depending on the viscosity of the polymer melt at a certain temperature, it would be also possible to use polymers with a higher T_g for MEW printing. The critical values that need to be tested in advance are the degradation temperature of the drug and the viscosity of the polymer melt at a certain temperature. The limitation of the polymer melt viscosity could be overcome by addition of a plasticiser, which could decrease the viscosity.

4. Conclusion

In this study, a highly water-soluble ABA triblock copolymer, comprising 2-methyl-2-oxazine as A blocks and 2-pentyl-2-oxazoline as block B, was successfully synthesized and blended via hot melt extrusion with indomethacin as model drug resulting in extrudates with different polymer:IND ratios of 2:1, 1:1 and 1:2 (w/w). Remaining crystallinity after HME of IND within the extrudates was visible but could potentially be removed by optimizing HME parameters. However, the remaining crystallinity of the drug was overcome by using MEW as a 3D printing technology, enabling the fabrication of microfibrous scaffolds with high porosity and therefore, improved surface area favourable for a fast dissolution of the polymer and drug release. Furthermore, MEW is a multi-parameter process leading to the advantage of adjustable scaffold design and therefore, the drug-loading content within the scaffold.

Taken together, this study introduces a new potential polymer excipient enabling amorphous blends with high levels of amorphous drugs for drug delivery applications. Due to the living cationic ring-opening polymerisation, the polymer can be easily modulated depending on the requirements. In combination with MEW, highly porous fibrous scaffolds can be fabricated without the need of a toxic solvent and with high precision of fiber placement offering a wide range of designs for further applications, even beyond sublingual drug delivery approaches.

Conflict of Interest Statement

The authors declare the following potential conflicts of interest(s): R.L. is listed as inventors on patents and patent applications pertinent to some materials discussed in this contribution and is co-founder of DelAQUA Pharmaceuticals, intend on commercialization of poly(2-oxazoline) based drug formulations.

Author contributions

Conceptualization and study design: L.K., Z.M., J.C.K., R.L.. Polymer synthesis and characterization: L.K.. Formulation preparation and characterization: L.K., Z.M., J.C.K.. Data acquisition and analysis: L.K., Z.M., J.C.K.. Writing and revising of manuscript: L.K., Z.M., J.C.K., R.L.. Funding acquisition: R.L., J.C.K.. All authors have read and agreed to the published version of the manuscript.

Acknowledgement

The authors would like to gratefully acknowledge the financial support by Academy of Finland (Grant No. 337660) and Volkswagen Foundation (Grant No. 93418). J.C. Kade is additionally supported by the Joachim Herz Foundation and appreciates financial support from Erasmus+ Traineeship Programme, as well as the Bavarian State Ministry of Science and the Arts and the University of Würzburg to the Graduate School of Life Sciences (GSLS), University of Würzburg, Germany. Authors' grateful thanks are also extended to Prof. Dietmar Hutmacher and Peter Bate for their support in providing the custom-built MEW.
Furthermore, the (technical) assistance of Sami-Pekka Hirvonen for SEC, Sami Hietala for melt rheology and Heikki Räikkönen for PXRD measurements is appreciated.

References

(1) Hoffmann, E. M.; Breitenbach, A.; Breitkreutz, J. Advances in orodispersible films for drug delivery. *Expert opinion on drug delivery* **2011**, *8* (3), 299-316.
(2) Li, J.; Pan, H.; Ye, Q.; Shi, C.; Zhang, X.; Pan, W. Carvedilol-loaded polyvinylpyrrolidone electrospun nanofiber film for sublingual delivery. *Journal of Drug Delivery Science and Technology* **2020**, *58*, 101726.
(3) Ibrahim, M. S.; Elsayyad, N. M. E.; Salama, A.; Noshi, S. H. Quality by design (qbd) as a tool for the optimization of indomethacin freeze-dried sublingual tablets: in vitro and in vivo evaluation. **2021**.
(4) Labhade, S.; Malode, C.; Rawal, V.; Rupvate, S. Review on Sublingual Drug Delivery System. *Journal of Drug Delivery and Therapeutics* **2019**, *9* (3), 684-688.
(5) Munjal, A.; Allam, A. E. Indomethacin. In *StatPearls [Internet]*, StatPearls Publishing, 2021.
(6) Gliszczyńska, A.; Nowaczyk, M. Lipid formulations and bioconjugation strategies for indomethacin therapeutic advances. *Molecules* **2021**, *26* (6), 1576.
(7) Hu, C.; Zhang, F.; Fan, H. Evaluation of Drug Dissolution Rate in Co-amorphous and Co-crystal Binary Drug Delivery Systems by Thermodynamic and Kinetic Methods. *AAPS PharmSciTech* **2021**, *22* (1), 1-9.
(8) Moseson, D. E.; Parker, A. S.; Beaudoin, S. P.; Taylor, L. S. Amorphous solid dispersions containing residual crystallinity: Influence of seed properties and polymer adsorption on dissolution performance. *European Journal of Pharmaceutical Sciences* **2020**, *146*, 105276.
(9) Bhujbal, S. V.; Mitra, B.; Jain, U.; Gong, Y.; Agrawal, A.; Karki, S.; Taylor, L. S.; Kumar, S.; Zhou, Q. Pharmaceutical amorphous solid dispersion: A review of manufacturing strategies. *Acta Pharmaceutica Sinica B* **2021**, *11* (8), 2505-2536.
(10) Jelić, D.; Liavitskaya, T.; Vyazovkin, S. Thermal stability of indomethacin increases with the amount of polyvinylpyrrolidone in solid dispersion. *Thermochimica Acta* **2019**, *676*, 172-176.

(11) Browne, E.; Worku, Z. A.; Healy, A. M. Physicochemical properties of poly-vinyl polymers and their influence on ketoprofen amorphous solid dispersion performance: a polymer selection case study. *Pharmaceutics* **2020**, *12* (5), 433.
(12) Fael, H.; Ràfols, C.; Demirel, A. L. Poly(2-Ethyl-2-Oxazoline) as an Alternative to Poly(Vinylpyrrolidone) in Solid Dispersions for Solubility and Dissolution Rate Enhancement of Drugs. *Journal of Pharmaceutical Sciences* **2018**, *107* (9), 2428-2438.
(13) Edueng, K.; Mahlin, D.; Bergström, C. A. The need for restructuring the disordered science of amorphous drug formulations. *Pharmaceutical research* **2017**, *34* (9), 1754-1772.
(14) Lübtow, M. M.; Keßler, L.; Appelt‐Menzel, A.; Lorson, T.; Gangloff, N.; Kirsch, M.; Dahms, S.; Luxenhofer, R. More Is Sometimes Less: Curcumin and Paclitaxel Formulations Using Poly (2‐oxazoline) and Poly (2‐oxazine)‐Based Amphiphiles Bearing Linear and Branched C9 Side Chains. *Macromolecular bioscience* **2018**, *18* (11), 1800155. Haider, M. S.; Luxenhofer, R. Development of Poly (2-oxazoline) s and poly (2-oxazine) s based formulation library and estimation of polymer/drug compatibility. **2022**.
(15) Lübtow, M. M.; Lorson, T.; Finger, T.; Gröber‐Becker, F. K.; Luxenhofer, R. Combining ultra‐high drug‐loaded micelles and injectable hydrogel drug depots for prolonged drug release. *Macromolecular Chemistry and Physics* **2020**, *221* (1), 1900341. Luxenhofer, R.; Sahay, G.; Schulz, A.; Alakhova, D.; Bronich, T. K.; Jordan, R.; Kabanov, A. V. Structure-property relationship in cytotoxicity and cell uptake of poly (2-oxazoline) amphiphiles. *Journal of Controlled Release* **2011**, *153* (1), 73-82. Seo, Y.; Schulz, A.; Han, Y.; He, Z.; Bludau, H.; Wan, X.; Tong, J.; Bronich, T. K.; Sokolsky, M.; Luxenhofer, R. Poly (2‐oxazoline) block copolymer based formulations of taxanes: effect of copolymer and drug structure, concentration, and environmental factors. *Polymers for Advanced Technologies* **2015**, *26* (7), 837-850.
(16) Sedlacek, O.; Bardoula, V.; Vuorimaa‐Laukkanen, E.; Gedda, L.; Edwards, K.; Radulescu, A.; Mun, G. A.; Guo, Y.; Zhou, J.; Zhang, H. Influence of Chain Length of Gradient and Block Copoly (2‐oxazoline) s on Self‐Assembly and Drug Encapsulation. *Small* **2022**, *18* (17), 2106251. Sedlacek, O.; Hoogenboom, R. Drug Delivery Systems Based on Poly (2‐oxazoline) s and Poly (2‐oxazine) s. *Advanced Therapeutics* **2020**, *3* (1), 1900168. Vlassi, E.; Papagiannopoulos, A.; Pispas, S. Amphiphilic poly(2-oxazoline) copolymers as self-assembled carriers for drug delivery applications. *European Polymer Journal* **2017**, *88*, 516-523.
(17) Luxenhofer, R.; Schulz, A.; Roques, C.; Li, S.; Bronich, T. K.; Batrakova, E. V.; Jordan, R.; Kabanov, A. V. Doubly amphiphilic poly (2-oxazoline) s as high-capacity delivery systems for hydrophobic drugs. *Biomaterials* **2010**, *31* (18), 4972-4979. Zahoranová, A.; Luxenhofer, R. Poly (2‐oxazoline)‐and Poly (2‐oxazine)‐Based Self‐Assemblies, Polyplexes, and Drug Nanoformulations—An Update. *Advanced Healthcare Materials* **2021**, *10* (6), 2001382. Chroni, A.; Mavromoustakos, T.; Pispas, S. Poly (2-oxazoline)-Based Amphiphilic Gradient Copolymers as Nanocarriers for Losartan: Insights into Drug–Polymer Interactions. *Macromol* **2021**, *1* (3), 177-200.
(18) Anane-Adjei, A. B.; Jacobs, E.; Nash, S. C.; Askin, S.; Soundararajan, R.; Kyobula, M.; Booth, J.; Campbell, A. Amorphous solid dispersions: Utilization and challenges in preclinical drug development within AstraZeneca. *International Journal of Pharmaceutics* **2021**, 121387.
(19) Modica de Mohac, L.; Keating, A. V.; de Fátima Pina, M.; Raimi-Abraham, B. T. Engineering of nanofibrous amorphous and crystalline solid dispersions for oral drug delivery. *Pharmaceutics* **2018**, *11* (1), 7.
(20) Davoodi, P.; Lee, L. Y.; Xu, Q.; Sunil, V.; Sun, Y.; Soh, S.; Wang, C.-H. Drug delivery systems for programmed and on-demand release. *Advanced drug delivery reviews* **2018**, *132*, 104-138.

(21) Qi, S.; Craig, D. Recent developments in micro-and nanofabrication techniques for the preparation of amorphous pharmaceutical dosage forms. *Advanced Drug Delivery Reviews* **2016**, *100*, 67-84.
(22) Kade, J. C.; Dalton, P. D. Polymers for melt electrowriting. *Advanced Healthcare Materials* **2021**, *10* (1), 2001232. Robinson, T. M.; Hutmacher, D. W.; Dalton, P. D. The next frontier in melt electrospinning: taming the jet. *Advanced Functional Materials* **2019**, *29* (44), 1904664.
(23) Florczak, S.; Lorson, T.; Zheng, T.; Mrlik, M.; Hutmacher, D. W.; Higgins, M. J.; Luxenhofer, R.; Dalton, P. D. Melt electrowriting of electroactive poly (vinylidene difluoride) fibers. *Polymer International* **2019**, *68* (4), 735-745.
(24) Youssef, A.; Hrynevich, A.; Fladeland, L.; Balles, A.; Groll, J.; Dalton, P. D.; Zabler, S. The impact of melt electrowritten scaffold design on porosity determined by x-ray microtomography. *Tissue Engineering Part C: Methods* **2019**, *25* (6), 367-379.
(25) Meng, J.; Boschetto, F.; Yagi, S.; Marin, E.; Adachi, T.; Chen, X.; Pezzotti, G.; Sakurai, S.; Yamane, H.; Xu, H. Design and manufacturing of 3D high-precision micro-fibrous poly (l-lactic acid) scaffold using melt electrowriting technique for bone tissue engineering. *Materials & Design* **2021**, *210*, 110063.
(26) Bai, J.; Wang, H.; Gao, W.; Liang, F.; Wang, Z.; Zhou, Y.; Lan, X.; Chen, X.; Cai, N.; Huang, W. J. I. j. o. p. Melt electrohydrodynamic 3D printed poly (ε-caprolactone)/polyethylene glycol/roxithromycin scaffold as a potential anti-infective implant in bone repair. **2020**, *576*, 118941.
(27) Witte, H.; Seeliger, W. Simple synthesis of 2‐substituted 2‐oxazolines and 5, 6‐dihydro‐4H‐1, 3‐oxazines. *Angewandte Chemie International Edition in English* **1972**, *11* (4), 287-288.
(28) Lübtow, M. M.; Hahn, L.; Haider, M. S.; Luxenhofer, R. Drug specificity, synergy and antagonism in ultrahigh capacity poly (2-oxazoline)/poly (2-oxazine) based formulations. *Journal of the American Chemical Society* **2017**, *139* (32), 10980-10983.
(29) Wunner, F. M.; Bas, O.; Saidy, N. T.; Dalton, P. D.; Pardo, E. M. D.-J.; Hutmacher, D. W. Melt electrospinning writing of three-dimensional poly (ε-caprolactone) scaffolds with controllable morphologies for tissue engineering applications. *JoVE (Journal of Visualized Experiments)* **2017**, (130), e56289.
(30) Schindelin, J.; Arganda-Carreras, I.; Frise, E.; Kaynig, V.; Longair, M.; Pietzsch, T.; Preibisch, S.; Rueden, C.; Saalfeld, S.; Schmid, B. Fiji: an open-source platform for biological-image analysis. *Nature methods* **2012**, *9* (7), 676-682.
(31) Sedlacek, O.; Lava, K.; Verbraeken, B.; Kasmi, S.; De Geest, B. G.; Hoogenboom, R. Unexpected reactivity switch in the statistical copolymerization of 2-oxazolines and 2-oxazines enabling the one-step synthesis of amphiphilic gradient copolymers. *Journal of the American Chemical Society* **2019**, *141* (24), 9617-9622. Saegusa, T.; Kobayashi, S.; Nagura, Y. Isomerization polymerization of 1, 3-oxazine. IV. Kinetic studies on the polymerization of 2-methyl-5, 6-dihydro-4H-1, 3-oxazine. *Macromolecules* **1974**, *7* (6), 713-716.
(32) Wu, Y.; Hu, J.; Zhang, C.; Han, J.; Wang, Y.; Kumar, B. A facile approach to fabricate a UV/heat dual-responsive triple shape memory polymer. *Journal of Materials Chemistry A* **2015**, *3* (1), 97-100.
(33) Huang, D.; Xie, Z.; Rao, Q.; Liamas, E.; Pan, P.; Guan, S.; Zhang, Z. J.; Lu, M.; Li, Q. Hot melt extrusion of heat-sensitive and high melting point drug: Inhibit the recrystallization of the prepared amorphous drug during extrusion to improve the bioavailability. *International journal of pharmaceutics* **2019**, *565*, 316-324.
(34) S'ari, M.; Blade, H.; Cosgrove, S.; Drummond-Brydson, R.; Hondow, N.; Hughes, L. P.; Brown, A. Characterization of amorphous solid dispersions and identification of low levels of crystallinity by transmission electron microscopy. *Molecular Pharmaceutics* **2021**, *18* (5), 1905-1919.
(35) Mahieu, A. l.; Willart, J.-F. o.; Dudognon, E.; Danède, F.; Descamps, M. A new protocol to determine the solubility of drugs into polymer matrixes. *Molecular pharmaceutics* **2013**, *10* (2), 560-566.
(36) Gupta, P.; Bansal, A. K. Molecular interactions in celecoxib-PVP-meglumine amorphous system. *Journal of pharmacy and pharmacology* **2005**, *57* (3), 303-310.

(37) Nahm, D.; Weigl, F.; Schaefer, N.; Sancho, A.; Frank, A.; Groll, J.; Villmann, C.; Schmidt, H.-W.; Dalton, P. D.; Luxenhofer, R. A versatile biomaterial ink platform for the melt electrowriting of chemically-crosslinked hydrogels. *Materials Horizons* **2020**, *7* (3), 928-933.
(38) Li, J.; Li, L.-B.; Nessah, N.; Huang, Y.; Hidalgo, C.; Owen, A.; Hidalgo, I. J. Simultaneous analysis of dissolution and permeation profiles of nanosized and microsized formulations of indomethacin using the in vitro dissolution absorption system 2. *Journal of Pharmaceutical Sciences* **2019**, *108* (7), 2334-2340.
(39) Shimada, Y.; Komaki, H.; Hirai, A.; Goto, S.; Hashimoto, Y.; Uchiro, H.; Terada, H. Decarboxylation of indomethacin induced by heat treatment. *International Journal of Pharmaceutics* **2018**, *545* (1-2), 51-56.
(40) Lopez, F. L.; Shearman, G. C.; Gaisford, S.; Williams, G. R. Amorphous Formulations of Indomethacin and Griseofulvin Prepared by Electrospinning. *Molecular Pharmaceutics* **2014**, *11* (12), 4327-4338. DOI: 10.1021/mp500391y.
(41) El-Badry, M.; Fetih, G.; Fathy, M. Improvement of solubility and dissolution rate of indomethacin by solid dispersions in Gelucire 50/13 and PEG4000. *Saudi Pharmaceutical Journal* **2009**, *17* (3), 217-225.

Supporting information

Using Melt Electrowriting to Prepare Highly Porous Microfiber Scaffolds of Amorphous Solid Dispersions of Indomethacin

Larissa Keßler[1], Zeynab Mirzaei[1], Juliane C. Kade[1, 2, 3], Robert Luxenhofer[1*]

L. Keßler, Z. Mirzaei, J. C. Kade, R. Luxenhofer

[1] Soft Matter Chemistry, Department of Chemistry, and Helsinki Institute of Sustainability Science, Faculty of Science, University of Helsinki, 00014 Helsinki, Finland

J. C. Kade

[2] Polymer Functional Materials, Chair for Advanced Materials Synthesis, Department of Chemistry and Pharmacy, Julius-Maximilians-University Würzburg, Würzburg, Germany.

J. C. Kade

[3] Department for Functional Materials in Medicine and Dentistry at the Institute of Functional Materials and Biofabrication, Julius-Maximilians-University Würzburg, Pleicherwall 2, 97070 Würzburg, Germany

Monomer Synthesis

2-methyl-2-oxazine (MeOzi)

Table S1. Chemicals used for the monomer synthesis of 2-methyl-2-oxazine (MeOzi).

reagent	equ.	molar mass [g mol^{-1}]	n [mol]	mass [g]
acetonitrile	1	41.05	2.5219	104
aminopropanol	1.20	75.11	3.0263	227
zincacetate dihydrate	0.025	219.51	0.063	14
MeOzi	1	99.13	2.5219	250

Yield: 97.25 g (38.9%, 0.981 mol)

NMR: (CD_2Cl_2; 500 MHz; 298 K) δ [ppm] = 4.141 - 4.037 (t, 2H, H^1, ^3J = 5.484 Hz); 3.313 - 3.183 (t, 2H, H^2, ^3J = 5.624 Hz); 1.839 - 1.717 (m, 5H, H^3).

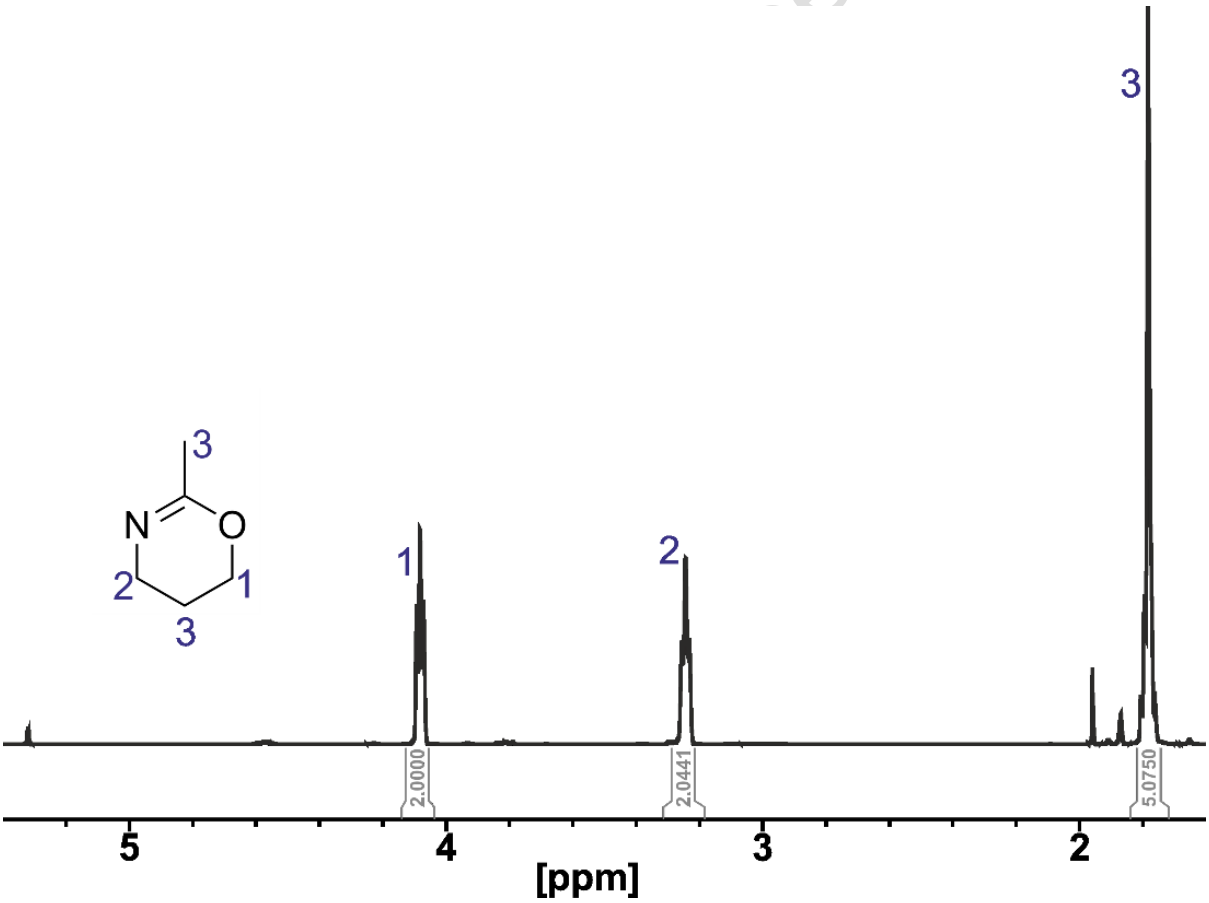

Figure S1. ^{1}H-NMR (500 MHz, 298 K, CD_2Cl_2) of the 2-methyl-2-oxazine (MeOzi).

2-pentyl-2-oxazoline (PentOx)

Table S2. Chemicals used for the monomer synthesis of 2-pentyl-2-oxazoline (PentOx).

reagent	equ.	molar mass [g mol^{-1}]	n [mol]	mass [g]
hexanenitrile	1	97.16	0.6232	61
aminoethanol	1.20	61.08	0.7478	46
zincacetate dihydrate	0.025	219.51	0.0156	3
PentOx	1	141.21	0.6232	88

Yield: 54.73 g (62.19%, 0.380 mol)

NMR: (CD_2Cl_2; 500 MHz; 298 K) δ [ppm] = 4.225 – 4.088 (t, 2H, H^1, ^3J = 9.437 Hz); 3.803 – 3.676 (t, 2H, H^2, ^3J = 9.013 Hz); 2.264 – 2.147 (t, 2H, H^3, ^3J = 7.654 Hz); 1.686 - 1.495 (pent, 2H, H^4, ^3J = 7.470 Hz); 1.372 - 1.230 (m, 4H, H^5); 0.946 - 0.809 (m, 3H, H^6).

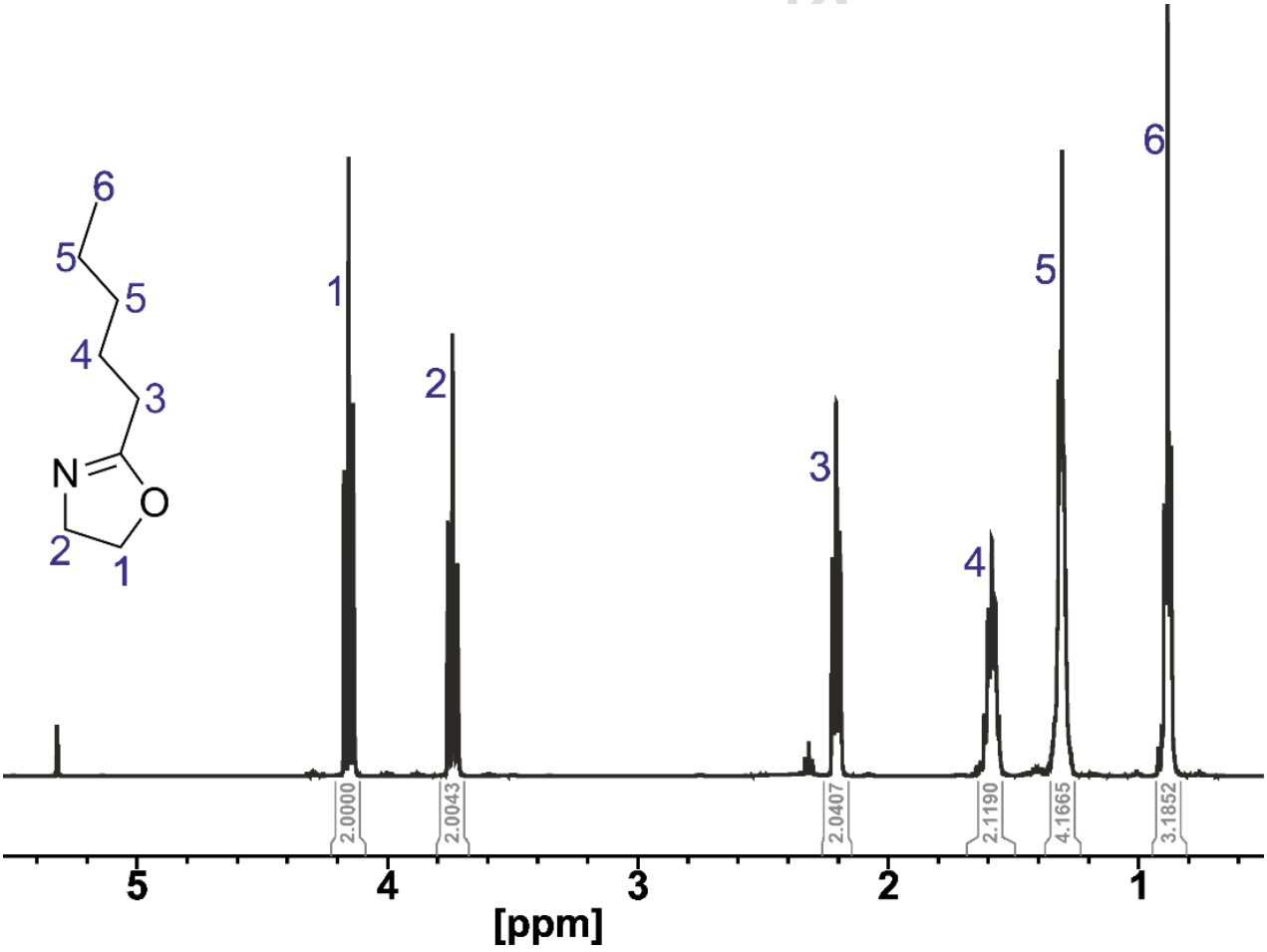

Figure S2. ^{1}H-NMR (500 MHz, 298 K, CD_2Cl_2) of the 2-pentyl-2-oxazoline (PentOx).

Polymer Synthesis

pMeOzi-b-pPentOx-b-pMeOzi

Table S3. Chemicals used for the polymer synthesis of MeOzi-PentOx-MeOzi.

reagent	equ.	molar mass [g mol^{-1}]	n [mol]	mass [g]
bromomethylbenzene	1	171.04	0.0107	1.84
MeOzi 1st block	35	99.13	0.3762	37.29
PentOx 2nd block	15	141.21	0.1612	22.76
MeOzi 3rd block	35	99.13	0.3762	37.29
ethyl isonipecotate	3	157.21	0.0322	5.07
pMeOzi-b-pPentOx-b-pMeOzi	1	9304.6	0.0107	100

Benzonitrile (4 M): 224 mL

Yield: 92.34 g (92.34%, 9.924 mmol)

$M_{w,theor.}$: 9304.6 g mol^{-1}

SEC (DMF): M_n = 6.8 kg mol^{-1}, Đ = 1.45

NMR: M_n = 12.6 kg mol^{-1}
Benz-pMeOzi$_{41}$-b-pPentOx$_{30}$-b-pMeOzi$_{41}$-PipCOOEt:
(CD_2Cl_2; 500 MHz; 298 K) δ [ppm] = 7.406 – 7.168 (m, 5H, H^1); 3.513 – 3.360 (br, 118H, H^2); 3.353 – 3.178 (br, 327H, H^3); 2.370 – 2.178 (br, 60H, H^4); 2.128 – 1.968 (br, 253H, H^5 and H_2O); 1.898 – 1.680 (br, 247H, H^6); 1.639 – 1.498 (br, 65H, H^7); 1.388 – 1.229 (br, 122H, H^8); 0.944 – 0.851 (br, 88H, H^9).

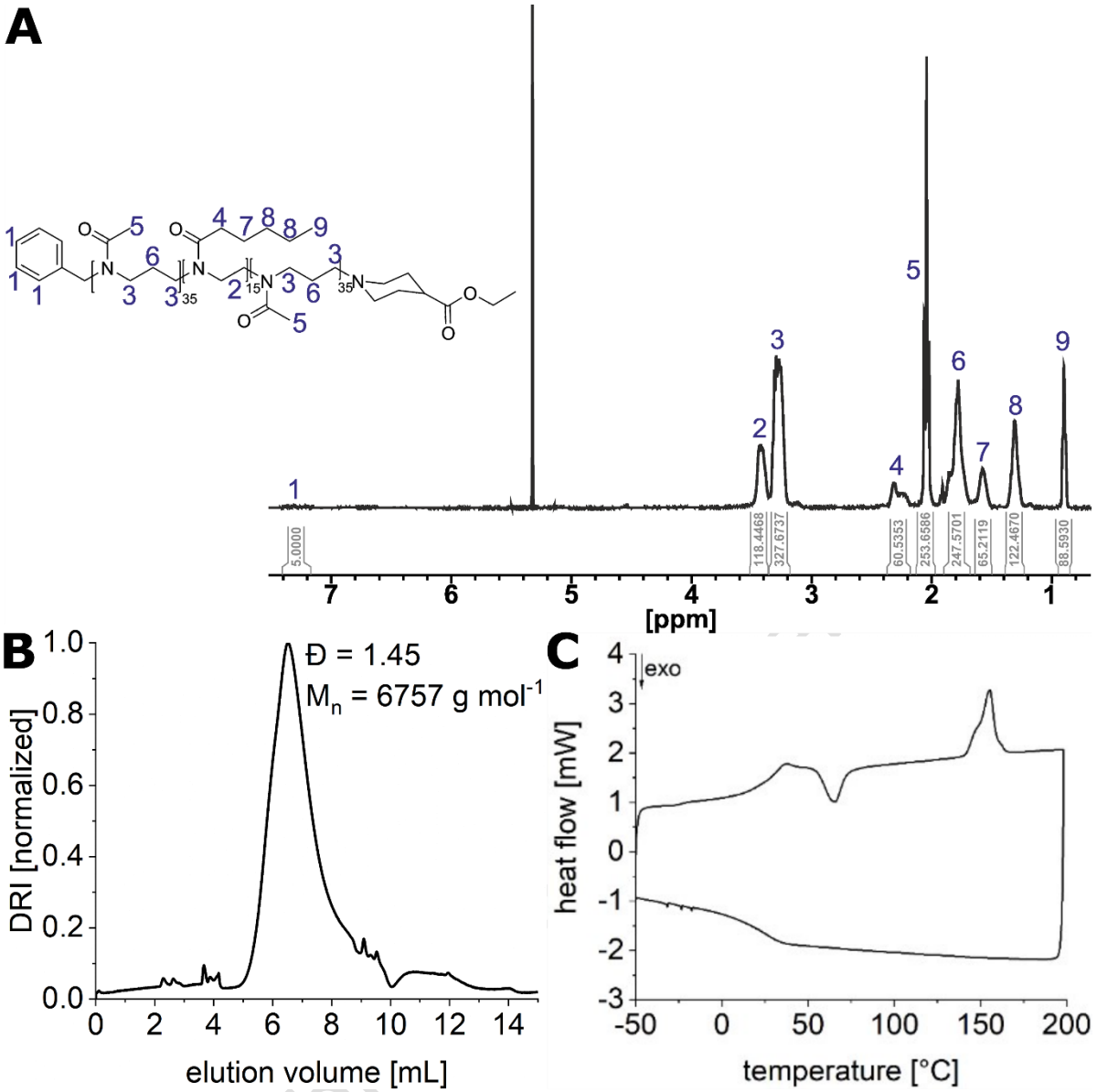

Figure S3. Showing the A) ^{1}H NMR spectrum (500 MHz, 298 K, CD_2Cl_2), B) SEC measurement (DMF) and C) DSC thermogram indicating the 2nd heating and cooling curves of the ABA triblock copolymer, comprising poly-2-methyl-2-oxazine as block A and poly-2-pentyl-2-oxaxoline as block B.

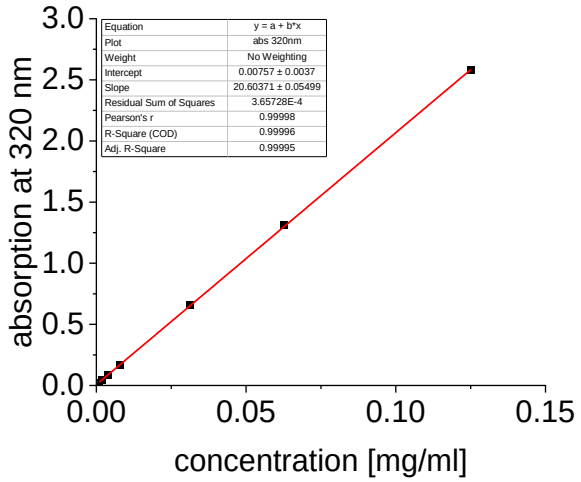

Figure S4. IND standard curved measured at a wavelength of 320 nm for corresponding UV-Vis measurements.

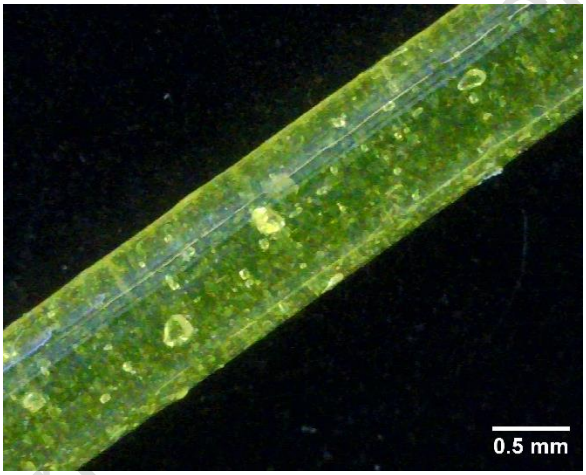

Figure S5. Microscope images of the resulting extrudates with polymer:IND w/w ratio of 1:1 indicating the remaining crystallinity of the incorporated IND after HME.

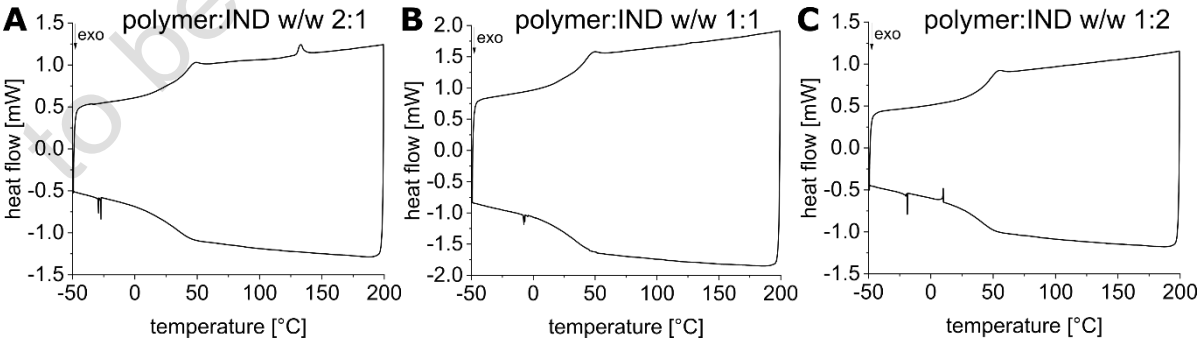

Figure S6. DSC thermograms of the extrudates indicating the 2nd heating and cooling curves of polymer:IND w/w A) 2:1, B) 1:1 and C) 1:2 extrudates.

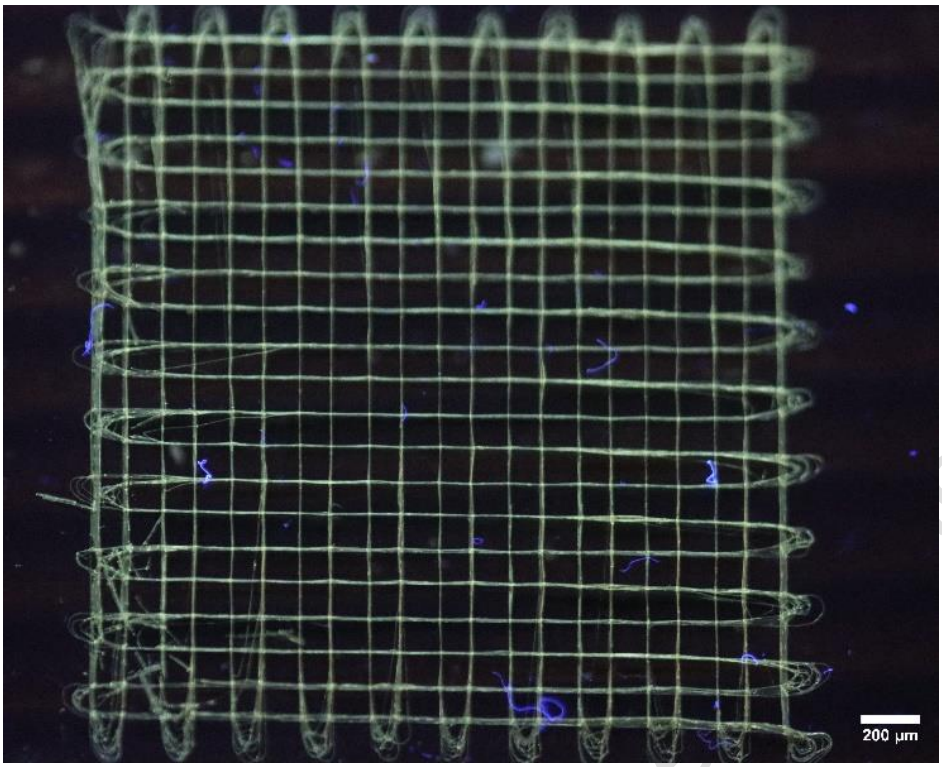

Figure S7. Image MEW scaffold with the polymer:IND w/w ratio of 1:1 under the UV light showing homogenous distribution of IND within the scaffold.

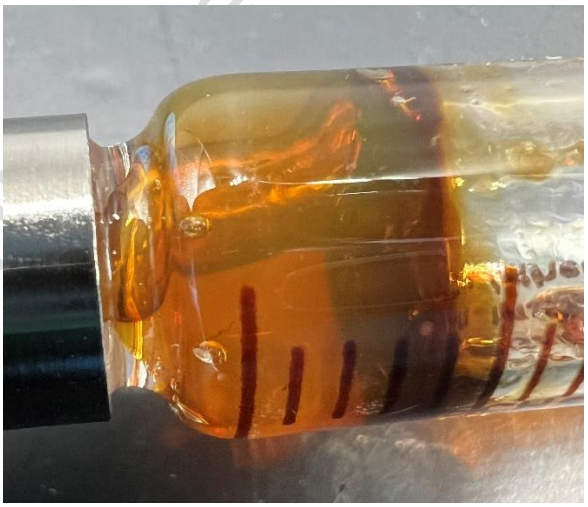

Figure S8. Photograph of the syringe used for MEW processing indicating the colour change of the polymer:IND w/w 2:1 on the top of the polymer melt and therefore, the degradation of the drug processed at 140°C, over a printing time of several hours.

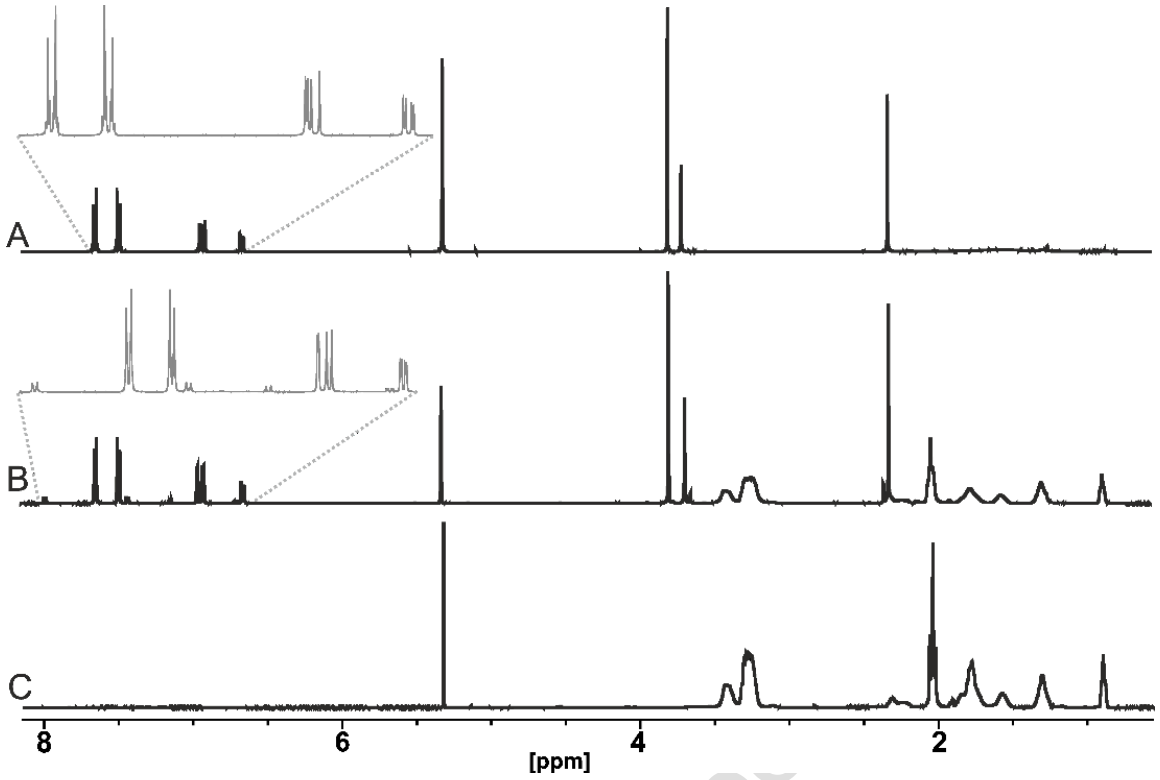

Figure S9. ^{1}H NMR (500 MHz, 298 K, CD_2Cl_2) of A) indomethacin, B) the extrudate with polymer:IND w/w ratio of 1:2 after heating at 140°C for several hours within the syringe reservoir in the printer and C) neat polymer.